Preface

This preface presents the sixth edition of our remote sensing text. During the interval that has elapsed since our fifth edition, the pace of remote sensing has increased in several respects, expanding the scope of our text and presenting new content. The advanced capabilities of satellite systems, thermal imagery, and drones have made essential contributions to our efforts to address the significant challenges of our time, including wildfires, floods, and coastal erosion. Few could have anticipated the development of analytical tools and techniques that are now available for analysis of remotely sensed data, the explosion of new sensor systems, or the multiplicity of remote sensing's applications throughout society. Such developments alone present challenges for any text on this subject.

Our sixth edition benefits from the addition of a new author, Dr. Valerie Thomas, an experienced faculty member at Virginia Tech, who now joins Dr. Randolph Wynne and Dr. James Campbell. Dr. Thomas brings new knowledge and perspectives to the text that will benefit users at all levels.

Changes in our field have also been reflected in the new four-color design throughout, with hundreds of new photos and figures, including original drawings by Susmita Sen. In addition, there are three new chapters on remote sensing platforms, agriculture, and forestry. Technological advances and cutting-edge applications are presented throughout this volume, including (1) discussions of Landsat 8 and Sentinel-2, (2) the growth of unmanned aerial systems, (3) mobile data collection, (4) current directions in climate change detection, (5) fire monitoring, (6) disaster response, and many other timely topics.

With the use of varied local and global examples and case studies, this sixth edition will provide readers with an understanding of the latest tools and principles of collecting remote images, analyzing and interpreting the images, and applying them to land and water use. It shows how remote sensing data are used in multiple fields, including plant sciences, agriculture, forestry, earth sciences, hydrology, and land-use analysis.

WHO THIS BOOK IS FOR

We wrote this text as a two-in-one book that will provide students with an accessible introduction to remote sensing, which can also serve as a foundational reference book. For students who intend to specialize in remote sensing, this text forms not only an introduction but also a framework for subjects to be studied in greater detail. Students who do plan specialization in remote sensing should consult their instructors to plan a comprehensive course of study based on work in several disciplines, as discussed in Chapter 1. This approach is presented in the text itself, introducing students to the principal topics of significance for remote sensing, but acknowledging that students will require additional depth in their chosen fields of specialization.

For those students who do not intend to pursue remote sensing beyond the introductory level, our text serves as an overview and introduction, so that they can understand remote sensing, its applications in varied disciplines, and its significance in today's world. For many, the primary emphasis will likely be on study of the chapters and methods of greatest significance in the student's major field of study.

SPECIAL FEATURES TO AID READERS

The chapters now open with a list of the chapter's major topics, and, as mentioned earlier, new case examples, such as Washington State's Oso River debris flow, illustrate each chapter's concepts. Chapters conclude with end-of-chapter review questions on the chapter's content. And, for many chapters, we have added a short list of teaching and learning resources—principally a selection of online tutorials or short videos, such as those found on YouTube; these videos provide depth or breadth to the content presented in the chapter or simply illustrate content. They have been selected for their brevity (most are less than 3–4 minutes or so in length) and for their effectiveness in explaining or illustrating content relative to the chapter in question. For the most part, we have excluded videos that focus on promotional content. Those videos that do serve a promotional purpose have been selected for their effectiveness in presenting technical content rather than as an endorsement of a particular product or service.

ORGANIZATION

We have retained the popular short-chapter format used in previous editions that can be taught in any order to meet the specific needs of each instructor. Numbered sections within chapters form smaller units that instructors can select and combine with other content as preferred. Our content provides organization at several levels to encourage instructors to select specific structures for their courses. At the broadest level, the rough division into four units offers a progression in the knowledge presented, with occasional concessions to practicality (such as placing the "Image Interpretation" chapter in Part II under "Image Acquisition" rather than in its logical position in Part III, "Analysis"). Here, we present each division as consisting of three or more chapters organized as follows:

Part I. Foundations
- Chapter 1. Introducing Remote Sensing Basics
- Chapter 2. Electromagnetic Radiation
- Chapter 3. Remote Sensing Platforms

Part II. Image Acquisition
- Chapter 4. Digital Mapping Cameras
- Chapter 5. Digital Imagery
- Chapter 6. Image Interpretation
- Chapter 7. Land Observation Satellites
- Chapter 8. Active Microwave
- Chapter 9. Lidar
- Chapter 10. Thermal Imagery

Part III. Analysis
- Chapter 11. Statistics and Preprocessing
- Chapter 12. Image Classification
- Chapter 13. Accuracy Assessment
- Chapter 14. Hyperspectral Remote Sensing
- Chapter 15. Change Detection

Part IV. Applications
- Chapter 16. Plant Science Fundamentals
- Chapter 17. Agricultural Remote Sensing
- Chapter 18. Forestry
- Chapter 19. Earth Sciences
- Chapter 20. Coastal Processes and Landforms
- Chapter 21. Land Use and Land Cover

NEW TO THIS EDITION

Now in full color with over 400 figures, hundreds of which are new to this edition, this sixth edition includes the latest technological advances and cutting-edge applications throughout. Three new chapters have been added, and they cover remote sensing platforms, agriculture, and forestry. Additional updates by chapter include:

Chapter 1. Introducing Remote Sensing Basics: A new section introduces both workers who contributed to the basics of aviation and those who have advanced worldwide achievements. This chapter also includes updated coverage of Open Landsat data policy, unmanned aerial vehicles (UAVs), and thermal infrared sensors (TIRS) thermal imaging.

Chapter 3. Remote Sensing Platforms: This new chapter introduces readers to fundamental aspects of remote sensing, including aerial cameras, Landsat imagery, unmanned aerial systems (UASs), tethered balloons used in the monitoring of wildlife, satellite systems (including geofencing), and mobile collection of field data (such as cell phones).

Chapter 7. Land Observation Satellites: This chapter describes the most recent Landsat system, Sentinel-2A and 2B, from the European Space Agency, and SPOT 7 (a French satellite), which provides information for land management, disaster response, and security programs.

Chapter 9. Lidar: Lidar (*light detection and ranging*) systems record the intensity and timing of returns from a pulsed laser. Airborne laser scanning systems often use near-infrared lasers to map the elevation of land surfaces in fine detail. New coverage includes lidar pulse densities, the normalized point cloud, lidar profiles, point clouds derived using digital aerial photogrammetry, heights extracted from waveforms, and lidar data collected from the International Space Station (ISS).

Chapter 10. Thermal Imagery: This chapter provides new examples of aerial images depicting thermal features, such as the heating of urban landscapes or forest fires (such as those within the Shasta-Trinity Forest); thermal images of residential structures; urban heat islands; and daytime/nighttime satellite imagery.

Chapter 11. Statistics and Preprocessing: In the context of digital analysis of remotely sensed data, preprocessing refers to those operations that are preliminary to the principal analysis. Thus, preprocessing forms a preparatory phase that, in principle, improves image quality as the basis for later analyses that will extract information from the image. New content includes expanded coverage of principal components analysis (PCA), image statistics, and conversion to top- or bottom-of-atmosphere reflectance.

Chapter 12. Image Classification: This chapter has been almost completely rewritten to include modern machine learning approaches that have largely supplanted Bayesian maximum likelihood. These include *k*-nearest neighbor, classification trees, and random forests.

Chapter 13. Accuracy Assessment: This chapter now reflects current best practices, including guiding the user step-by-step through probabilistic sampling design, computing and reporting area proportions in the area matrix, and using the area proportions in summary statistics like the overall accuracy, user's accuracy, and producer's accuracy.

Chapter 14. Hyperspectral Remote Sensing: This chapter now includes common processing protocols like the spectral hourglass and their component steps (e.g., locating and identifying endmembers and spectral unmixing).

Chapter 15. Change Detection: This chapter has been updated to include a typology of multitemporal change detection techniques and details of common algorithms such as exponentially weighted moving average change detection and continuous change detection and classification. Change attribution is also explicitly addressed.

Chapter 16. Plant Science Fundamentals: Expanded discussion of leaf or canopy water content has been added, along with indices appropriate for their estimation. The land surface phenology section has been updated and expanded. Methods for the remote estimation of chlorophyll and solar-induced fluorescence have been detailed.

Chapter 17. Agricultural Remote Sensing: This new chapter shows how remote sensing's aerial perspective provides significant insights into agricultural landscapes. It includes coverage of analytical strategies for agricultural analysis of satellite imagery, irrigated agriculture, crop calendars, storm-damaged crops, tillage status, agricultural management, and the USDA cropland data layer.

Chapter 18. Forestry: Forestry's wide-ranging management objectives—including timber, forest products, water quality, carbon, sequestration, biodiversity, and wildlife conservation—are explored in this new chapter. Other topics include the assessment of competing vegetation, species identification, forest photogrammetry, airborne laser scanning, fire fuel loading, and forest measurements and monitoring.

Chapter 19. Earth Sciences: This chapter examines terrain, physiography, and geomorphic systems in an Earth systems context, with new coverage of major landslides (Oso, Washington, and Grand Mesa, Colorado); examples of stream diversion (northwestern Virginia); soil mapping; and soil scientists.

Chapter 20. Coastal Processes and Landforms: New topics include multispectral bathymetry, wave generation, swash and backwash, beach profiles (Virginia's barrier islands), coastal classification (Texas Point), storm damage (Mantoloking, New Jersey), and renewal (Miami Beach).

ACKNOWLEDGMENTS

We gratefully acknowledge the contributions of those who assisted in the work on this book, especially Dr. Susmita Sen, who devoted special attention to create 81 new valuable graphics for our sixth edition. We also acknowledge the support of Kathryn Hollandsworth (Virginia Tech), who reviewed, corrected, and edited text that benefited from her careful attention. We note also the contributions of Michelle Klopfer and Stacy Kuhar, both of whom supported our project. We also recognize the assistance of several colleagues, who provided graphics, insight, and information that were sometimes acquired at remote locations. Among these colleagues were Dr. Baojuan Zheng, Dr. Tammy Parece, Dr. Hoa Tran, Dr. Iris Fynn, and Dr. Jie Ren, who all provided useful and insightful content that contributed significantly to our project over long intervals. Other students who contributed include Robert Severynse, Austin Hays, Michael Graham, Jessica Dorr, and Eric Guenther.

We would also like to thank past instructors and students who made suggestions for earlier editions of this book and for the sixth edition, including eight initially anonymous Guilford reviewers whose identities have recently been revealed to us: Nate Currit, Texas State University; Mary Henry, Miami University, Oxford; Anthony Filippi, Texas A & M University; Robert A. Washington-Allen, University of Tennessee, Knoxville; Jeffrey Chambers, University of California–Berkeley; Greg Gaston, University of North Alabama; Andrew Klein, Texas A & M University; and Eric S. Kasischke, University of Maryland.

And at The Guilford Press, Seymour Weingarten, Editor-in-Chief, has continued his support of our project over our six editions, with the support of Guilford and its many members. C. Deborah Laughton, Publisher in Methodology and Senior Editor in Geography, has been an essential partner in producing this project and supporting us through challenging conditions. We specifically recognize the role of Katherine Sommer for her strong editorial support, organizing the final manuscript, tracking down figures and their permissions, and finding alternatives when needed. Robert Sebastiano, also at Guilford, was available to assist with a variety of permissions questions and tasks.

9 Lidar

MAJOR TOPICS TO UNDERSTAND

- Profiling Lasers
- Scanning (Imaging) Lidars
- Types of Lidar
- Lidar Data
- Selected Lidar Applications
- Lidar Data Formats

9.1 INTRODUCTION

Lidar (*light detection and ranging*) is an active ***remote sensing*** system (i.e., a system that can generate energy [light] to assess ground features). Lidars generate pulsed laser light that can measure distances and generate precise, three-dimensional data describing the Earth and its surface features.

Functional components of a lidar system include (1) a laser scanner, (2) a Global Positioning System (GPS) with its associated highly accurate clock, and (3) an inertial navigation system (INS), typically mounted on aircraft. The laser scanner transmits brief laser pulses to the surface (up to about 300,000 per second), which are scattered back to the laser scanner. As the system receives returning pulses from the surface, it records the time interval required to reach the surface and return. The system can then calculate, for each pulse, the distance between the laser scanner and the surface. Lidars can use ultraviolet, visible, or near-infrared light to scan objects. Near-infrared and green wavelengths are most commonly used for the systems discussed in this chapter.

Lidar can be considered as a technology analogous to radar imagery, in the sense that both families of sensors are designed to transmit energy in a narrow range of frequencies, then receive backscattered energy to form images of the Earth's surface. Both classes of instruments are active sensors; that is, they provide their own sources of energy, which means they are independent of solar illumination. More importantly, both have characteristics of transmitted and returned energy (i.e., the timing of pulses, wavelengths, and angles), so that they can be used to assess not only the brightness of backscattered energy, but also its angular position, changes in frequency, and timing of reflected pulses. Such knowledge means that lidar data, much like data acquired by active microwave sensors, permit extraction of information describing terrain, structures, vegetative features, and other features not recorded by optical sensors.

Lidars are based on an application of *lasers,* using a form of *coherent* light—light that is composed of a very narrow band of wavelengths—very "pure" with respect to color. Whereas ordinary light (even if it transmits a specific color) is composed of many wavelengths, with a diverse assemblage of waveforms, a laser produces light that is in phase ("coherent"), comprised of a narrow range of wavelengths ("monochromatic") (Figure 9.1). Such light can be transmitted over large distances as narrow beams that will diverge only slightly, in contrast to light we observe in our everyday experience that disperses over distance.

The laser—an acronym for light amplification by stimulated emission of radiation—is an instrument that applies a strong electrical current to a "lasable" material, usually crystals or gases, such as rubies, CO_2, helium–neon, argon, and other less familiar materials. Such *lasable* materials have atoms, molecules, or ions that emit light as they return to a normal ground state after excitement by a stimulus, such as electricity or light. The emitted light forms the coherent beam described above. Each separate material provides a specific laser with its distinctive characteristics with respect to wavelength.

The laser provides an intense beam that does not diverge as it travels from the transmitter, a property that can favor applications involving heating, cutting, etching, or illu-

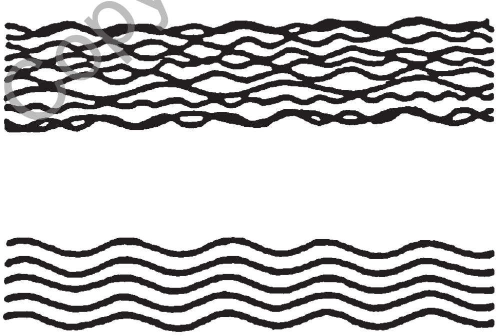

FIGURE 9.1 Normal (top) and coherent (bottom) light.

mination. Laser pointers, laser printers, CD players, scanners, bar code readers, and many other everyday consumer items are based on laser technology. Although imaging lasers do not use intense beams, they do exploit the focused, coherent nature of the beam to produce focused light. A laser uses mirrored surfaces to accumulate many pulses to increase the intensity of the light before it leaves the laser (Figure 9.2).

9.2 PROFILING LASERS

Lasers were invented in the late 1950s and were initially used for scientific inquiry and industrial applications. The first environmental uses of lidars were principally for *atmospheric profiling:* static lasers were mounted to point upward into the atmosphere to assess atmospheric aerosols. Solid particles suspended in the atmosphere directed a portion of the laser beam back to the ground, where its density indicated the abundance of atmospheric particles. Because lasers can measure the time delay of the backscatter, they can assess the clarity of the atmosphere over a depth of several kilometers, providing a measure of atmospheric quality.

The first airborne lasers were designed as *profiling lasers*—lasers aimed directly beneath the aircraft to illuminate a single region in the nadir position. (When used primarily to acquire topographic data, such instruments are known as *airborne laser altimeters*.) Forward motion of the aircraft carries the illuminated region forward to view a single track directly beneath the aircraft. Echoes from repetitive lidar pulses provide an elevation profile of the narrow region immediately beneath the aircraft (Figure 9.3). Although lidar profilers do not provide the image formats that we now expect, they provide a high density of observations and are used as investigative tools for researchers investigating topography, vegetation structure, hydrography, and atmospheric studies, among many applications.

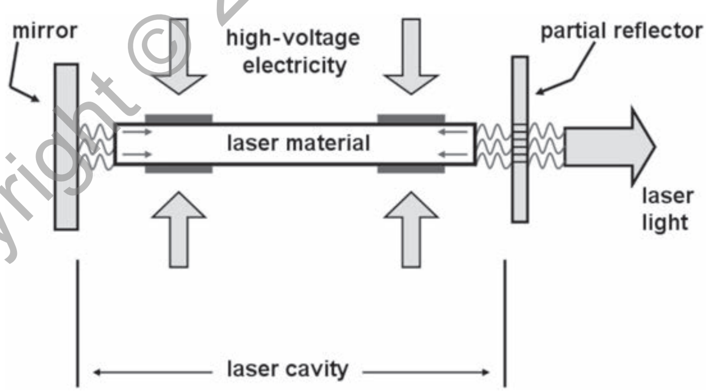

FIGURE 9.2 Schematic diagram of a simple laser. Energy, such as electricity, is applied to a substance, such as lasable gases (e.g., nitrogen, helium, neon) or materials (e.g., ruby crystals). When the materials return to their normal state, they emit coherent light, which is intensified before release by multiple reflections between the mirrored surfaces. Intensified light can then pass through the semitransparent mirror to form the beam of coherent light that is emitted by the instrument.

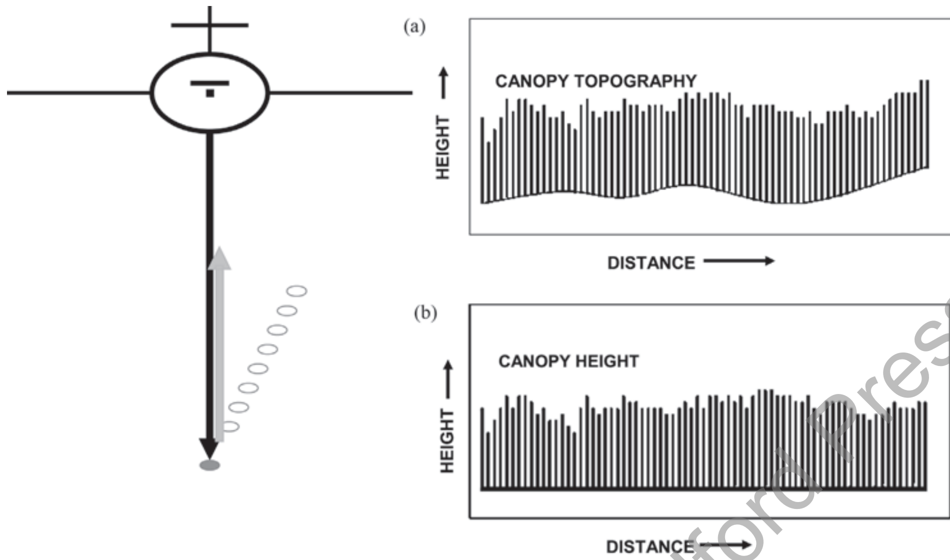

FIGURE 9.3 Schematic representation of an airborne laser profiler. (a) Acquisition of laser profile; (b) sample data gathered by a laser profiler, illustrating extraction of canopy height from the raw profile data.

9.3 SCANNING (IMAGING) LIDARS

By the late 1980s, several technologies matured and converged to create the context for development of precision scanning lidar systems that we now know. In this context, lidars assumed their current role as remote sensing instruments tailored for collection of imagery of the Earth's surface. *Inertial measurement units* (IMUs) enabled precise control and recording of orientation of aircraft (roll, pitch, and yaw). GPS could provide accurate records of geographic location of an aircraft as it acquired data. Furthermore, development of highly accurate clocks permitted the precise timing of lidar pulses required to create high-performance lidar scanning systems.

A lidar scanner can transmit up to 300,000 pulses per second, depending on the specific design and application. A scanning mirror directs the pulses back and forth across the image swath beneath the aircraft. The width of the swath is determined by the instrument's design and the operating conditions of the aircraft. Most imaging lidars use wavelengths in the visible or near-infrared regions of the electromagnetic spectrum. Common near-infrared wavelengths include 1,024 or 1,064 nm, which are sensitive to vegetation, relatively free from atmospheric scattering, and are absorbed by open water. Green wavelengths (e.g., 532 nm) are more common for applications with ice and water.

Several alternative designs for imaging lidar instruments are in use (Habib, 2010). Figure 9.4 presents a schematic representation of a typical lidar system. (1) The system's laser (coordinated by the electronic component) generates a beam of coherent light, transmitted by a fiber optic cable to (2) a rotating mirror, offset to provide a scanning motion. The laser light is directed to fiber optic cables that can be twisted to transmit the light as a linear beam (3). The oscillating motion of the mirror scans the laser beam from side to side along the cross-track axis of the image, recording many thousands of returns each second. Because a lidar scanner is well integrated with GPS, IMUs, and timing systems, these pulses can be associated with specific points on the Earth's surface. As the reflected portion of the laser beam reaches the lidar aperture, it is received by another system of lenses (4) and channeled through fiber optic cables to another scanning lens. (5) It is then directed through an optical system to filter light before it is directed to (6) a receiving system to accept and direct the signal to the electronics components. The electronics coordinate timing of the pulses and permit matching of the signal with data from the inertial navigation system and GPS.

Together, such components permit the system to place each returned signal in its correct geographic position. Typically, two fiberglass bundles are configured to view the ground along a linear path. One transmits laser pulses, and an identical bundle receives the echoes. The system operates at such high speed that a large collection of pulses is received from each square meter on the terrain. The timing capability of the lidar scan permits accurate assessment of distance and elevation, which enables formation of an image with detailed and accurate representation of features in the scene.

9.4 TYPES OF LIDAR

There are two main types of lidar technology: analog and photon-counting technology. The vast majority of lidar data currently available comes from analog systems designed for terrain analysis. Both of these technologies can also be used for water-related analysis, referred to as bathymetric lidar. Most of the lidar systems designed for terrain analysis use laser energy from the NIR wavelengths (1,024 nm or 1,064 nm are common), although some do use green wavelengths.

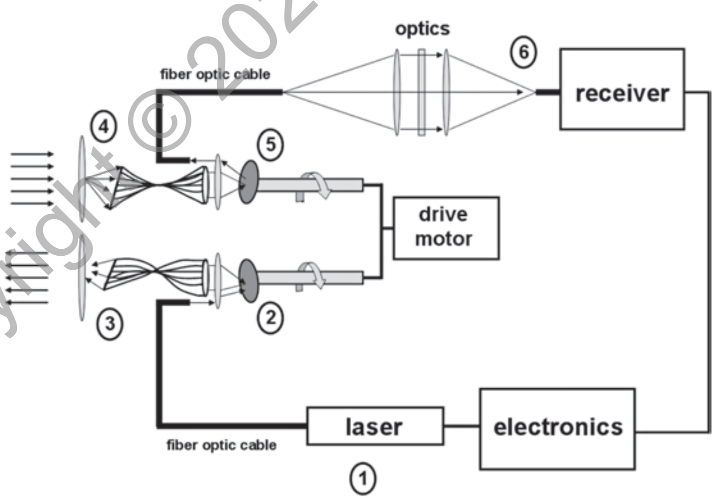

FIGURE 9.4 Schematic diagram of a lidar scanner. (1) The system's laser scanner (coordinated by the electronic component) generates a beam of light, transmitted by fiber optic cable to (2) a rotating mirror, offset to provide a scanning motion. The laser light is directed to a bundle of fiber optic cables that are twisted to provide a linear beam and then directed through a system of lenses toward the ground. The energy received back from the terrain is received by another system of lenses.

Analog Lidar

By far the most common type of lidar is analog lidar, where the returned lidar pulse is recorded as the amount of energy returned over time. Through processing, information about the speed of light, the scan angle, and the movement and orientation of the aircraft (made possible because of the GPS and IMU systems on the vehicle) are used to convert the data into elevation above the Earth's ellipsoid and the amount of energy returned from that elevation. These analog systems store the data as either the entire returned waveform, referred to as either *waveform lidar systems* or discrete returns (1, 2, or multiple returns) extracted at specific points within that waveform, referred to as *discrete lidar systems*. Most available lidar data today are from these analog systems, either waveform or discrete. The data are primarily collected from airborne systems, including UAVs, but they may also be collected from other vehicles, from backpack systems, or systems mounted on a tripod. These systems can collect profiles (typical of earlier lidar technology) or scans (most common today). Most of our discussion in this chapter refers to scanning analog system technology.

Photon-Counting Lidar

The second type of lidar system, referred to as photon-counting lidar, or quantum lid, uses quantum sensors to detect individual photons of light that are returned from the initial pulse. Photon-counting lidar has numerous technological advantages, with increased vertical sensitivity and the possibility of smaller instrumentation. However, the technology is relatively new, and there are far fewer systems with these types of data. One notable exception is the ATLAS instrument on the ICESat-2 satellite, which is designed to monitor ice sheet elevation and sea ice thickness. There are also a few airborne systems with this technology, which can provide data in incredible detail. However, because of the sensitivity of quantum sensors, the data tend to be very noisy, especially when collected from space, with significant returns from the atmosphere. This makes it difficult to use the data for the same types of land surface analysis that have become routine with analog lidar. Numerous ongoing research efforts are ongoing to remove the "noise" (unwanted returns) from the signal for specific applications. Because of the increased vertical sensitivity of these systems and the possibility for smaller instrumentation and other technological advantages, this type of lidar system will likely become prevalent in the coming years.

Bathymetric Lidar

Although bathymetric lidar is essentially the same technology we have described, the applications are very different. As discussed in Chapter 2, water typically absorbs most of the energy at the NIR wavelengths, so there are very few lidar returns from water if these wavelengths are used. However, as noted above, some systems use green light for the lidar energy (532 nm is common) or have multiple beams and capture both the green and NIR wavelength ranges. At green wavelengths, lidar can penetrate water, and so it may be used for bathymetric applications that capture the floor of the water body. Having both green and NIR wavelengths (typical for systems intended specifically for bathymetry) allows for the capture of the surrounding shoreline terrain and water surface (NIR) and bottom of the water body (green). Note that water penetration by bathymetric lidar is further discussed in Chapter 20.

9.5 LIDAR DATA

Lidar systems do not provide imagery in the same sense that we have been discussing with aerial photography, optical, or SAR sensors. Rather, they provide locations and ancillary data at each location, usually as discrete points or waveforms that describe some portion of the returned laser pulse recorded by the lidar system. In the case of scanning lidar systems, the data are so dense that it is common to convert either the height information or some of the ancillary information (e.g., the intensity of the return energy) into a high-resolution raster product and examine it with the same types of software programs used for other raster data. These products may be referred to as lidar imagery or a specific lidar-derived product.

Figure 9.5 provides a schematic sketch of a lidar system in flight, scanning side-to-side as the aircraft flies forward along its planned (linear) flight path. The noticeable V-shaped gaps occur because of the simultaneous forward motion of the aircraft (Figure 9.5, top). In reality, actual scan lines are positioned quite close together and frequently

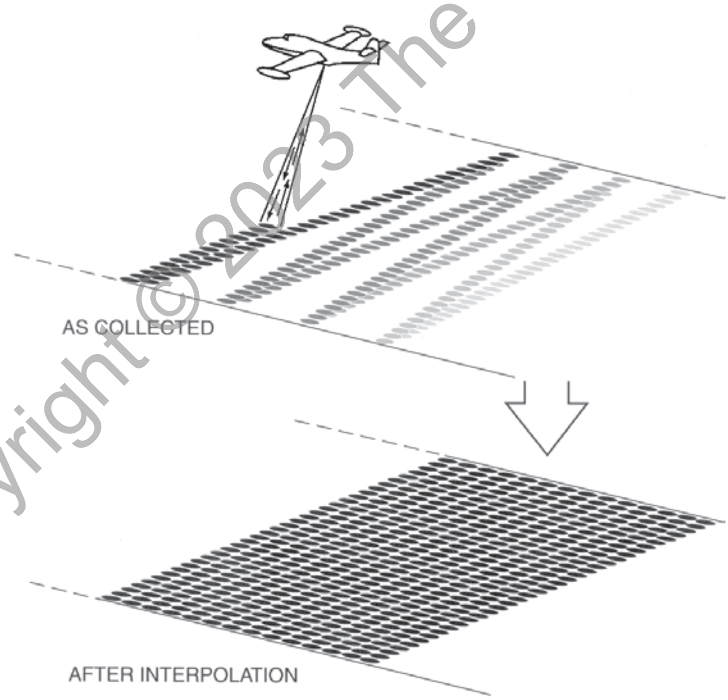

FIGURE 9.5 Acquisition of lidar data. Lidar systems acquire data by scanning in the patterns suggested by the top diagram; details vary according to specific systems. The pattern of returns can then be interpolated to generate a systematic array from the lidar data.

overlap with those of adjacent flight lines; they can be interpolated to form a dense, systematic array of pixels, as depicted in the lower section of Figure 9.5.

Discrete Analog Lidar Data

In the case of discrete lidar systems, each recorded lidar return can be precisely positioned in *xyz* space to provide a three-dimensional point cloud of position and associated attributes (intensity, scan angle, GPS time, etc.). The accuracy of these points will vary depending on the specifications of the system, which can be obtained from the manufacturer and the conditions on the ground. (*Note:* Forest cover and other conditions that cause GPS multipath errors can decrease locational point accuracy.) For small-footprint lidars (the most common type of lidar system), horizontal accuracy might be in the range of 20–30 cm, and vertical accuracy in the range of 15–20 cm. This enables the derivation of products from lidar data, such as digital elevation models of the ground surface, at comparable detail and positional accuracy to those acquired by photogrammetric analysis of aerial photographs.

The available terrain detail will vary based on the lidar pulse density. The lidar pulse rate refers to the number of laser pulses emitted by the lidar per second, which can be in the hundreds of thousands. This is dependent on the sensor specifications and has tended to increase over time, as technology improves. The pulse density refers to the number of lidar returns per unit of ground area and is dependent on many factors, including the pulse rate, altitude and speed of the plane, and the local terrain (Figure 9.6).

Within the lidar point cloud, *primary returns* (or *first returns*) originate from the first objects a lidar pulse encounters—which could be the upper surface of a vegetation canopy (Figure 9.6), buildings, objects, or the ground. In addition, portions of a pulse pass through gaps in the canopy or other pervious surfaces. Some of this energy may be returned from features within the encountered object (such as branches in a tree), of which some energy may eventually reach the ground. This energy creates echoes known as *secondary returns* (or *partial* or *multiple returns*). Therefore, for complex surfaces such as forests with multiple canopies, some portions of a pulse might be reflected from upper and middle portions of the canopy and other portions from the ground surface at the base (Figures 9.7 and 9.8).

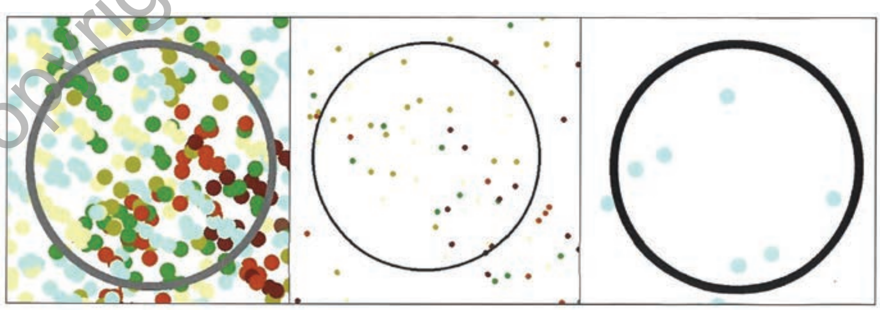

FIGURE 9.6 Representations of differing lidar pulse densities within a 1-m circle, illustrating variations in the objectives of the lidar mission. From Parece et al. (2016). Used by permission of *VirginiaView.net.*

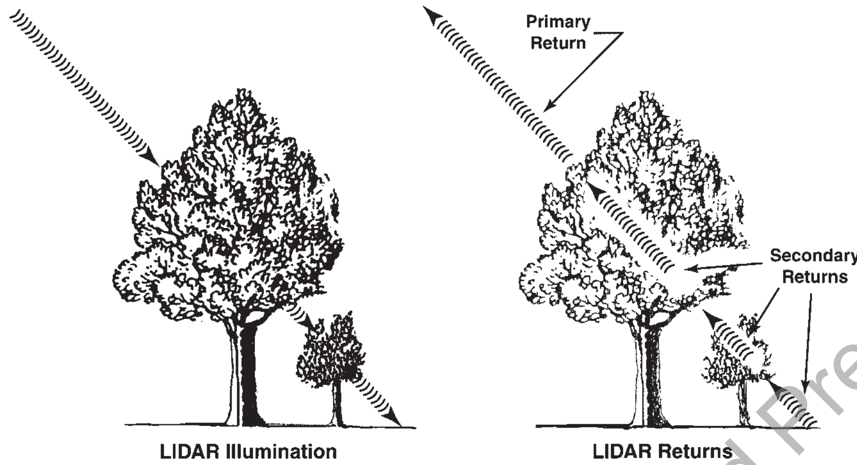

FIGURE 9.7 Schematic diagrams of primary and secondary lidar returns.

The resulting data is a three-dimensional point cloud (Figure 9.9). For some applications, particularly those related to vegetation analysis, researchers will analyze the point clouds themselves, to better understand the vertical distribution of points under different vegetation conditions (see Chapter 18). In the case of forest analysis, information such as canopy height, canopy openness, amount of leaf area, aboveground biomass, forest carbon, and other information about the physical shape and arrangement of the trees can be calculated from lidar point clouds.

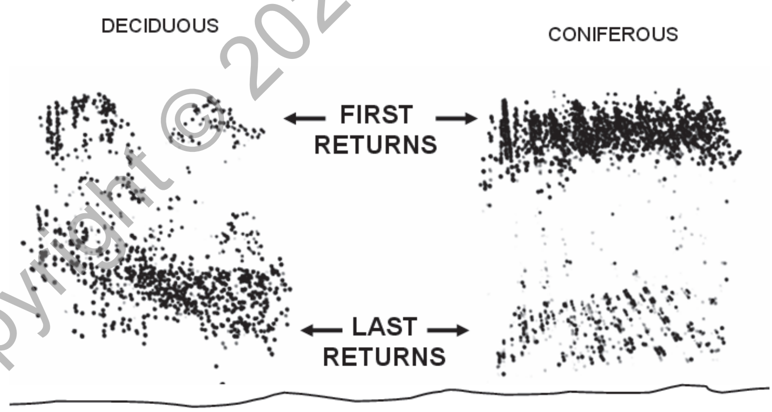

FIGURE 9.8 First and last lidar returns from a deciduous forest canopy (left) and a coniferous forest canopy (right), shown in a two-dimensional profile. Dots near the tops of the diagram represent returns that are received first (*primary returns*), when the pulse encounters the top or near the top of the forest canopy, and dots at the lower and central portions of the diagram represent returns received later (*secondary returns*). Note the contrast between dome-shaped canopies formed by crowns of the deciduous forest (left) and peaked crowns of the coniferous canopy (right). The coniferous forest has only sparse undergrowth, while the deciduous forest is characterized by abundant undergrowth. From Sorin Popescu. Used by permission.

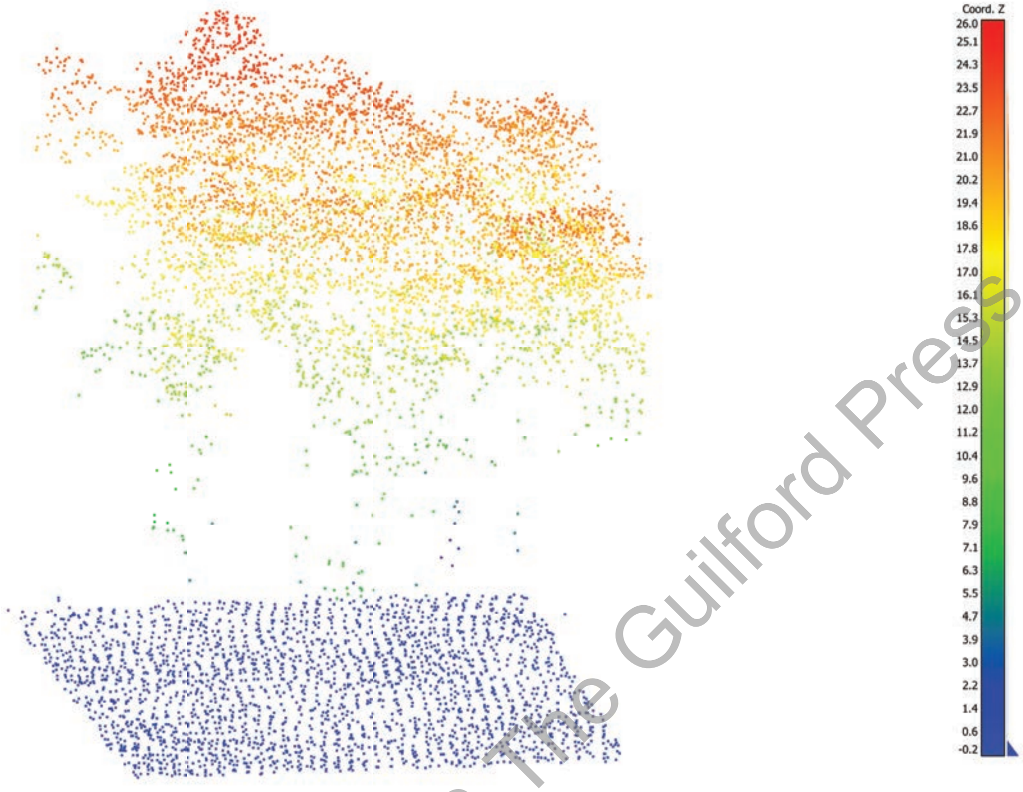

FIGURE 9.9 Normalized lidar point cloud for a deciduous forest. Ground level can be seen as dark blue points. Points at the top of the canopy are red. Normalization of the point cloud means that the ground elevation has been subtracted from all points in the cloud to remove the effect of terrain. The lidar is sourced from the National Ecological Observatory Network Mountain Lake Biological Station in Virginia. From Elizabeth M. Prior. Used by permission.

Figure 9.10 provides an example of a lidar profile (a slice extracted from the point cloud) of lidar data that contains multiple features of interest and illustrates the level of detail contained in the data. Details can be seen about the shape of individual tree crowns, the height and slope of building roofs, and the terrain along the profile. If desired, users can extract individual features and explore their shape in three dimensions, with measurements. In this example, the ground returns have been identified with a ground detection algorithm, and they are shown in brown. All other returns are white or gray.

Although the point cloud is useful for vegetation analysis, most applications of lidar data use raster-based products that are derived from the points through data processing. By far the most common product derived and used from lidar data is an interpolation of the ground returns to generate a digital elevation model (DEM) (Figure 9.11). Because lidar passes through vegetation and has high point density, lidar-derived DEMs have significant detail about the terrain surface and higher accuracy than other data sources that have been used in the past.

FIGURE 9.10 Example of a lidar profile. This lateral view depicts tree canopies, dwellings, and a gentle downhill slope left to right, revealing a slight variation in terrain relief. From Parece et al. (2016, pp. 159, 160). Used by permission of *VirginiaView.net*.

A closer view of the lidar-derived DEM from Figure 9.11 illustrates the detailed terrain information that is available with lidar data (Figure 9.12). Numerous details can be observed on the shaded relief of the surface, including a four-lane highway, nearby quarry, forested areas, and agricultural lands with a corn crop. Note that the data are detailed enough to show individual trees, including along a fence line (left side of the hillshade model). The parallel strips visible near the upper right depict mature cornfields—another example of the detail recorded by this technology.

Many applications use digital elevation models and topographic maps that existed long before lidar data became common. Some of these applications use ancillary information, such as contour lines, to provide information about topographic relief, slope, and aspect (Figure 9.13). There are industry standards with respect to the required accuracy of these products for topographic mapping. It is common practice to derive this ancillary information from lidar data during the data preprocessing stage and provide it as a product with the lidar data (at or exceeding required accuracy standards), even though the lidar data and the lidar-derived DEMs contain significantly more detail.

For urban applications, it is also common to extract information such as building footprints and their associated heights from the lidar first returns, in addition to providing the ground elevation in the DEM (Figure 9.14). It is also possible to generate an elevation model of the surface, which includes the heights of objects; these products are

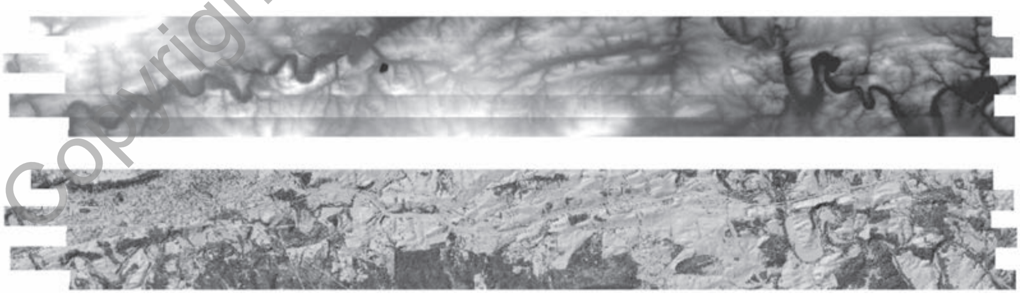

FIGURE 9.11 Top: Lidar-derived digital elevation model depicting terrain near Wytheville, Virginia, where brightness indicates relative elevation. Bottom: Lidar-derived shaded relief of the same area, generated using a hill-shading algorithm. This enables a view of the surface with shadow effects. From Virginia Department of Transportation. Copyright © 2003 Commonwealth of Virginia. Used by permission.

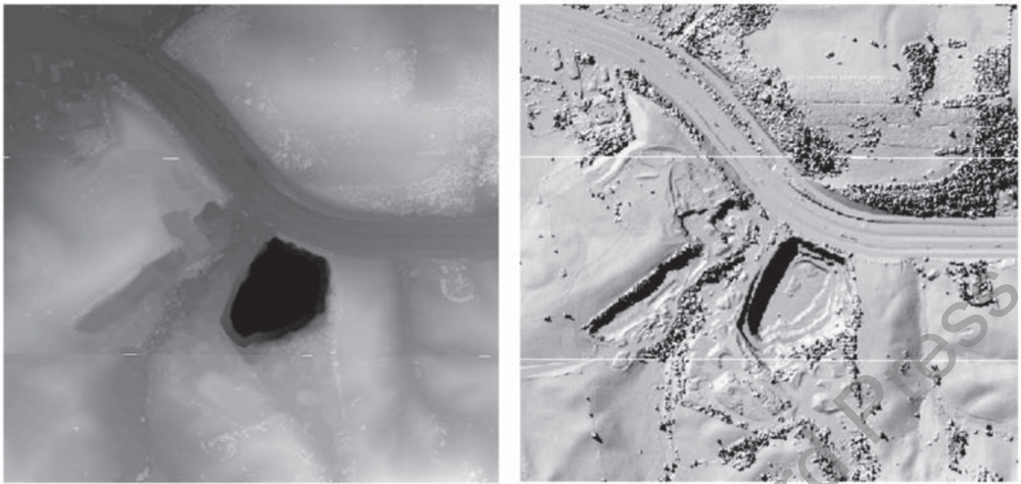

FIGURE 9.12 Portions of the lidar-derived DEM and hillshade model from **Figure 9.11** enlarged to depict detail. Left: The digital elevation model, with darker areas corresponding to lower elevation. Right: The hillshade model (or shaded relief) of the same area with shadow effects. Note the very fine spatial detail of the terrain, including individual trees and microtopography. From Virginia Department of Transportation. Copyright © 2003 Commonwealth of Virginia. Used by permission.

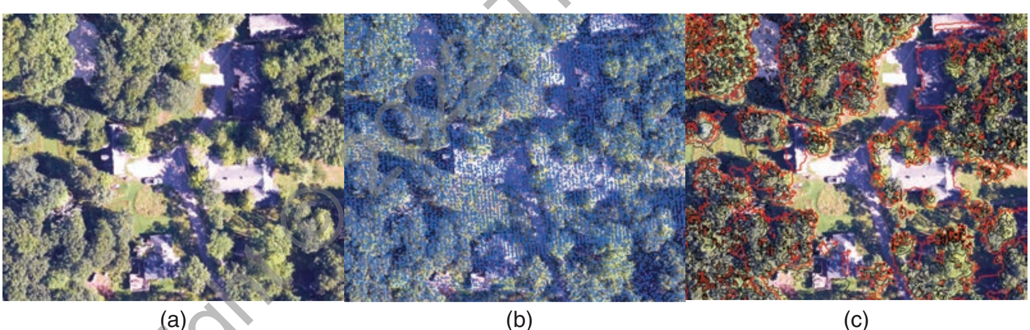

FIGURE 9.13 (a) High-resolution orthorectified camera imagery from 2015 of buildings and trees at the Mountain Lake Biological Station in Virginia. (b) Lidar last returns from 2015 (blue) displayed over the same imagery. Note the high density of points, which provides significant detail regarding three-dimensional structure. (c) 5-m contours derived from the last return points. Users can generate contours at intervals of their choice. Provisional data from National Ecological Observatory Network (2021a, 2021b).

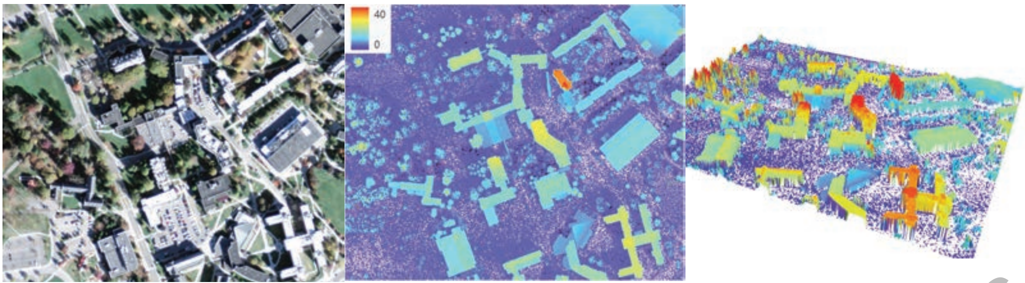

FIGURE 9.14 Left: Portion of a 2014 image from the U.S. Department of Agriculture National Agriculture Imagery Program (NAIP) over buildings on the Virginia Tech campus in Blacksburg, Virginia. Middle: A model of heights above ground (m) derived from lidar data. This model was created by subtracting a lidar-derived DSM from a lidar-derived DEM. The effects of terrain are removed, enabling the determination of feature heights, which include trees and buildings. Right: A three-dimensional viewing perspective of the same height model. From NAIP (left image). Middle and right image derived from 2017 lidar data provided by the USGS.

referred to as digital surface models (DSMs). Both DEMs and DSMs are raster products derived from lidar (similar to images) and are elevations relative to the Earth's ellipsoid. If they are subtracted, a third raster product will be generated that contains the heights above the ground.

Waveform Data

Waveform data provide significantly more information about the interaction of the lidar pulse with features on the surface. Although many systems collect waveform data, as a practical matter the applications for the waveform itself are relatively few other than for research. Instead, scientists have developed algorithms to process the raw lidar waveform and extract relative heights. Figure 9.15 shows a waveform of the boreal forest in northern Ontario, Canada, collected by the Global Ecosystem Dynamics Investigation (GEDI) profiling lidar that is currently operating from the International Space Station (ISS). The large spike in the waveform, near the bottom orange dashed line, represents the interaction of the waveform with the ground. The other nodes between the dashed lines characterize the vertical structure of the canopy (i.e., a representation of the trunks, branches, and foliage). Readers should keep in mind that this level of detail is available for all 470 samples that make up the graph in Figure 9.16. This information is valuable for scientists, particularly those who are interested in forest vertical structure and how it is changing.

Algorithms have been developed to identify heights that indicate a more significant return from a feature, referred to as relative heights (RH), where RH100 would represent the height of 100% aboveground energy return—in other words, the height of the top of a feature such as a forest canopy. RH0 would represent the ground, and RH25, RH50, and RH75 would represent some intermediate height, conceptually similar to multiple returns in the discrete systems described above. The algorithm used to process the waveform in Figure 9.15 identified the following relative heights, which are seen at sample number 442 in Figure 9.16: RH100 = 13.7 m (top orange dashed line in Figure 9.15);

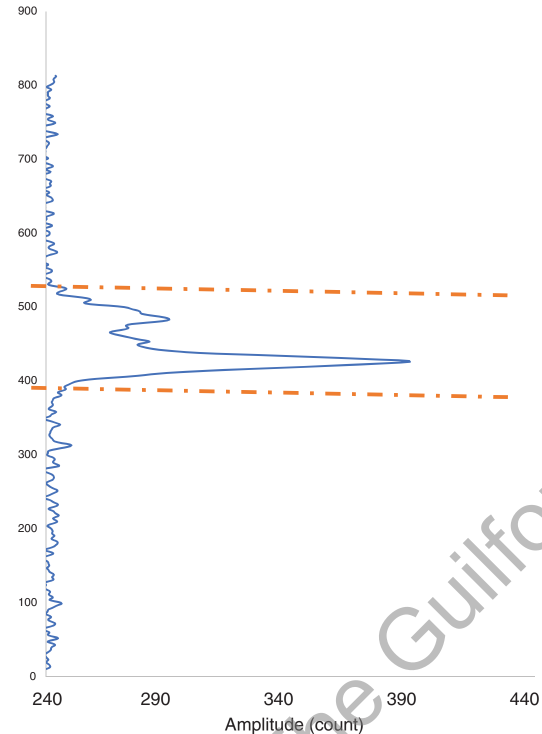

FIGURE 9.15 GEDI Level 1B RX waveform for sample 442 in **Figure 9.16**. The two dashed orange lines represent the approximate portion of the waveform that interacted with the boreal forest. The top orange dashed line represents the top of the canopy, at approximately 13.7 m above the ground. The largest spike in the waveform is caused by the ground, which causes the largest amount of energy return to the sensor. The signal above and below the dashed lines are considered background noise and are filtered out by the data processing algorithm.

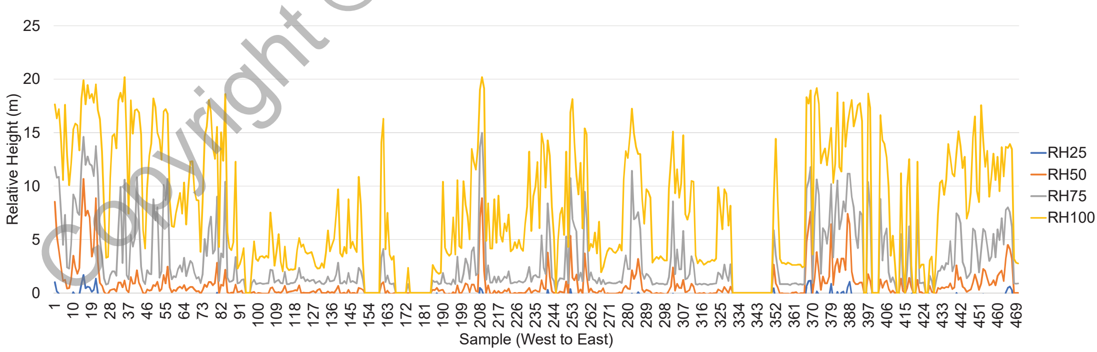

FIGURE 9.16 Example of relative heights extracted from waveform lidar collected by the GEDI system from the International Space Station (ISS) on August 7, 2019. The orbital path of the ISS passed over the boreal forest in northern Ontario, Canada. The graph shows the relative heights along a short transect, where each sample location on the graph can be linked to a full waveform, such as that in **Figure 9.15**. Available for public download in the GEDI level 2b data.

RH75 = 6.5 m; RH25 = 1.46 m. Users can obtain either the waveforms themselves or the processed relative heights, which are much easier to explore. In this example, RH25, RH50, RH75, and RH100 are shown along the profile, covering 470 individual waveform samples along the ISS ground track over northern Ontario. You can see that the top of the forest canopy is at or below 20 m (typical at this latitude), and there are areas along the transect that are relatively open, with much lower heights.

9.6 SELECTED LIDAR APPLICATIONS

From the beginning, lidar systems have been successfully applied to address an abundance of useful applications—essentially any application that benefits from height information, including detailed information about ground surface. Lidars have been effective in their ability to support varied functions under a range of conditions, including unfavorable weather, day/night conditions, and rough terrain. Common uses of lidar data include surveying, mapping of anthropogenic features, particularly urban, transportation, piping, and communication infrastructure, floodplain and flood risk mapping, archaeology, forestry (Chapter 18), coastal resilience (Chapter 20), agriculture, and bathymetry. There are many more uses of lidar data—too many to describe here. Below we expand upon four common terrain applications of lidar.

Forestry. Lidar data is used extensively in forestry, as it provides a method for characterizing tree size and shape, as well as the ground. This issue is discussed further in Chapter 18. Lidar is used to estimate canopy height, aboveground biomass, leaf area, and other forest inventory variables. Among other uses, this is important for forest industry, carbon monitoring, understanding biodiversity and wildlife habitat, mapping forested wetlands, predicting fire risk, and understanding hydrological processes in forests.

Agriculture. Monitoring agricultural lands is a critical component for a farmer's maintenance of agricultural productivity. Lidar observations provide an effective and inexpensive resource for monitoring crops during the growing season, supporting farmers' ability to closely monitor their crops, their status, and their yield. Lidar observations can also provide the basis for preparing topographic maps of fields in order to detect slopes, ponding, and erosion. Other types of remote sensing used for agriculture are described in more detail in Chapter 17.

Geology. Geoscientists have applied lidar imagery, often with GPS, to detect and interpret structural geology and geophysics to detect and study faults, as well as to measure uplift and other changes in terrain.

Archaeology. Lidar has made significant contributions to the detection and mapping of archaeological remains by revealing structures beneath forest canopies as well as the subtle outlines of building foundations, which are often buried but cause slight elevation changes detectable in the microtopography of a lidar-derived DEM. There have been dramatic archaeology finds in the rainforest, which is often too dense to penetrate with other forms of remote sensing. An example is the Mayan archaeology of Guatemala and Belize, where lidar revealed a much larger extent of civilization than had been previously known (e.g., Chase et al., 2014; Canuto et al., 2018).

9.7 LIDAR DATA FORMATS

As lidar technology has evolved and the data have become more available and heavily used, the way the data are stored has become more standardized. In early years, the data were often either in ASCII text format or in a proprietary binary format from the vendor. However, the ASCII format was impractical and computationally inefficient, and the proprietary formats were difficult to access. Over time, the binary LAS (LASer) file format became an industry standard, and it is now common to store the point and waveform in this format. The standards have evolved over time, as technology and data improved, and are specified by the American Society for Photogrammetry and Remote Sensing (ASPRS). Through each evolution (currently, version ASPRS LAS 1.4), consideration is given to legacy compatibility such that earlier lidar data can still be accessed. The format is designed to contain the data and the associated attributes. There is also the ability to store a reference class for each point, which can be assigned in postprocessing after the data are collected (ground, water, vegetation, etc.). The idea is that binary data are stored in a computationally efficient yet open and common format, around which software and analysis tools can be designed while still maintaining all-important attribute data for each point or waveform.

9.8 SUMMARY

Lidar provides a highly accurate, detailed representation of terrain and permits the separation of features (such as vegetation) from the terrain, a capability unique among remote sensing instruments. Its status as an active sensor permits convenience and flexibility in flight planning due to its insensitivity to variations in weather and solar illumination—both important constraints on aerial photography.

Lidar data provide detailed, spatial data of high accuracy and precision. Lidar gives a direct measurement of surface elevation, with detail and accuracy usually associated only with photogrammetric surveys. Some lidar applications replace photogrammetric applications of aerial photography. Many applications have focused on urban regions, which experience continuing needs for detailed information concerning building densities, urban structures, and building footprints. Lidar data are used for highway planning, pipeline routing, and design of wireless communication systems in urban regions. Although wall-to-wall lidar coverage of the United States does not exist, several states have completed or are planning to acquire statewide lidar coverage to support floodplain mapping programs and other efforts with broader geographic reach. Lidar data have also been used to study forest structure, as the detailed and accurate information describing canopy configuration and structure may permit accurate mapping of timber volume. There are now a broad range of environmental applications, in which lidar's detailed representations of terrain have opened avenues of inquiry that are not practical with coarser data. As lidar archives acquire increasing geographic scope and temporal depth, the field will be able to expand its reach to examine sequential changes in vegetation cover, land use, and geomorphology with a precision and accuracy not previously feasible.

SOME TEACHING AND LEARNING RESOURCES

Introductory Resources

- Introduction to Light Detection and Ranging (LiDAR)—Explore Point Clouds and Work with LiDAR Raster Data in R; National Ecological Observatory Network
  www.neonscience.org/intro-lidar-r-series
- Lidar: Light Detection and Ranging
  www.youtube.com/watch?v=hxiRkTtBQp8&fmt=22
- Parece, Tammy E., John A. McGee, and James B. Campbell. 2016. *Working with Lidar Using ArcGIS Desktop*. Blacksburg, VA: VirginiaView, 333 pp.
- 3D Elevation Program—United States Geological Survey (for publicly available lidar data)
  www.usgs.gov/core-science-systems/ngp/3dep

Examples of Lidar Data, Applications, and Acquisitions

- Lidar Surface Shadow Model for Boston's Back Bay
  www.youtube.com/watch?v=s4OhzaIXMhg&NR=1
- Pylon Lidar Survey
  www.youtube.com/watch?v=Dv6a0KgTbiw
- Terrapoint Aerial Services—Lidar Flight Simulation
  www.youtube.com/watch?v=GSPcyhSAgTQ&NR=1
- LandXplorer: Lidar Scan of London
  www.youtube.com/watch?v=F2xy-US46PQ&NR=1
- Lidar Survey
  www.youtube.com/watch?v=f1P42oQHN_M&feature=related
- eCognition Image Analysis: Extracting Tree Canopy from Lidar
  www.youtube.com/watch?v=OR1Se18Zd4E

REVIEW QUESTIONS

1. Review some of the strengths of lidar data relative to other forms of remotely sensed data discussed thus far.
2. Identify some reasons that lidar might be effectively used in combination with other data. What difficulties might be encountered in bringing together lidar data and, for example, fine-resolution optical satellite imagery?
3. Many observers believe that the increasing availability of lidar will displace the current role of aerial photography for many applications. What are some of the reasons that might lead people to believe that lidar could replace many of the remote sensing tasks now performed by aerial photography?
4. Can you identify reasons that aerial photography might yet retain a role, even in competition with the strengths of lidar data?

5. If aerial photography is largely replaced by lidar, do you believe that there will still be a role for teaching aerial photography as a topic in a university remote sensing course? Explain.
6. Assume for the moment that lidar data become much cheaper, easier to use, and, in general, more widely available to remote sensing practitioners. What kinds of new remote sensing analyses might become possible, or what existing analyses might become more widespread?
7. The text discusses how lidar data is based on the convergence of several technologies. Review your notes to list these technologies. Think about the technologic, scientific, social, and economic contexts that foster the merging of these separate capabilities. How do you think we can prepare to encourage future convergences of other technologies (now unknown) that might lead to advances in remote sensing instruments?
8. Lidar imagery may not be equally useful in all regions of the Earth. Can you suggest certain geographic regions or environments in which lidar data might not be effective?
9. Discuss some of the considerations that might be significant in deciding the season in which to acquire lidar data for your region.
10. Identify some of the special considerations that might be significant in planning acquisition of lidar data in urban regions.

REFERENCES

Blair, J. B., D. L. Rabine, and M. A. Hofton. 1999. The Laser Vegetation Imaging Sensor: A Medium-Altitude, Digitization-Only, Airborne Laser Altimeter for Mapping Vegetation and Topography. *ISPRS Journal of Photogrammetry and Remote Sensing*, Vol. 54, pp. 115–122.

Canuto, M. A., F. Estrada-Belli, T. G. Garrison, S. Houston, M. J. Acuña, M. Kováć, and D. Chatelain. (2018). Ancient Lowland Maya Complexity as Revealed by Airborne Laser Scanning of Northern Guatemala. *Science*, Vol. 361, No. 6409, p. eaau0137.

Chase, A. F., D. Z. Chase, J. J. Awe, J. F. Weishampel, G. Iannone, H. Moyes, . . . and M. K. Brown. (2014). The Use of LiDAR in Usnderstanding the Ancient Maya Landscape: Caracol and Western Belize. *Advances in Archaeological Practice,* Vol. 2, No. 3, pp. 208–221.

DeLoach, S. R., and J. Leonard. 2000. Making Photogrammetric History. *Professional Surveyor,* Vol. 20, No. 4, pp. 6–11.

Flood, M. 2001. Laser Altimetry: From Science to Commercial LiDAR Mapping. *Photogrammetric Engineering and Remote Sensing,* Vol. 67, pp. 1209–1217.

Flood, M. 2002. Product Definitions and Guidelines for Use in Specifying LiDAR Deliverables. *Photogrammetric Engineering and Remote Sensing,* Vol. 68, No. 12, pp. 1230–1234.

Habib, A. F. 2010. Airborne LIDAR Mapping. Chapter 23 in *Manual of Geospatial Science and Technology* (2nd ed.). (J. D. Bossler, ed.). Boca Raton, FL: CRC Press, pp. 439–465.

Hill, J. M., L. A. Graham, and R. J. Henry. 2000. Wide-Area Topographic Mapping Using Airborne Light Detection and Ranging (LIDAR) Technology. *Photogrammetric Engineering and Remote Sensing,* Vol. 66, pp. 908–914, 927, 960.

Hyyppä, J., W. Wagner, M. Hollaus, and H. Hyyppä. 2009. Airborne Laser Mapping. Chapter 14 in the *Sage Handbook of Remote Sensing* (T. A. Warner, M. D. Nellis, and G. M. Foody, eds.). London: SAGE, pp. 199–211.

Lefsky, M. A., D. Harding, W. B. Cohen, G. Parker, and H. H. Shugart. 1999. Surface Lidar Remote Sensing of Basal Area and Biomass in Deciduous Forests of Eastern Maryland, USA. *Remote Sensing of Environment,* Vol. 67, pp. 83–98.

National Ecological Observatory Network.2021a, July 28. Data Product DP1.30003.001, Discrete Return Lidar Point Cloud. Provisional data retrieved from *https://data.neonscience.org*.

National Ecological Observatory Network. 2021b, July 28. Data Product DP1.30010.001, High-Resolution Orthorectified Camera Imagery and Data Product DP1.30003.001, Discrete Return Lidar Point Cloud. Provisional data retrieved from *https://data.neonscience.org*.

Nelson, R., W. Krabill, and J. Tonelli. 1988a. Estimating Forest Biomass and Volume Using Airborne Laser Data. *Remote Sensing of Environment,* Vol. 24, pp. 247–267.

Nelson, R., R. Swift, and W. Krabill, W. 1988. Using Airborne Lasers to Estimate Forest Canopy and Stand Characteristics. *Journal of Forestry,* Vol. 86, pp. 31–38.

Nilsson, M. 1996. Estimation of Tree Heights and Stand Volume Using an Airborne Lidar System. *Remote Sensing of Environment,* Vol. 56, pp. 1–7.

Parece, T. E., J. A. McGee, and J. B. Campbell. 2016. *Working with Lidar Using ArcGIS Desktop.* Blacksburg, VA: VirginiaView, 333 pp.

Popescu, S. C. 2002. *Estimating Plot-Level Forest Biophysical Parameters Using Small-Footprint Airborne Lidar Measurements*. PhD Dissertation, Virginia Tech, Blacksburg, 144 pp.

Romano, M. E. 2004. Innovation in Lidar Processing. *Photogrammetric Engineering and Remote Sensing,* Vol. 70, pp. 1201–1206.

Sapeta, K. 2000. Have You Seen the Light? LIDAR Technology Is Creating Believers. *GEOWorld,* Vol. 13, No. 10, pp. 32–36.

Wehr, A., and U. Lohr (eds.). 1999. Airborne Laser Scanning: An Introduction and Overview. *ISPRS Journal of Photogrammetry and Remote Sensing,* Vol. 54, Nos. 2–3, pp. 68–82.

White, S. A., and Y. Wang. 2003. Utilizing DEMs Derived from LIDAR Data to Analyze Morphologic Change in the North Carolina Coastline. *Remote Sensing of Environment,* Vol. 85, pp. 39–47.

Zhang, K., and D. Whitman. 2005. Comparison of Three Algorithms for Filtering Airborne Lidar Data. *Photogrammetric Engineering and Remote Sensing,* Vol. 71, pp. 313–324.